

**Next Generation Vehicle Positioning Techniques for GPS-
Degraded Environments to Support Vehicle Safety and
Automation Systems**

FHWA BAA DTFH61-09-R-00004
EXPLORATORY ADVANCED RESEARCH PROGRAM

Auburn University
SRI (formerly Sarnoff)
The Pennsylvania State University
Kapsch TrafficCom Inc.
NAVTEQ North America LLC

Quarterly Report 7
April – June 2010

Table of Contents

1. SCOPE.....	3
1.1 SRI SARNOFF CONTRIBUTION.....	3
1.2 THE PENNSYLVANIA STATE UNIVERSITY CONTRIBUTION	4
1.3 KAPSCH TRAFFICCOM INC. CONTRIBUTION.....	4
2. CURRENT PROGRESS	4
2.1 SRI PROGRESS	4
2.1.1 <i>Visual Navigation Sensor Package and Data Collection</i>	4
2.1.2 <i>Extended Kalman Filter Model</i>	5
2.2 PENN STATE PROGRESS	7
2.2.1 <i>Real-time Implementation</i>	7
2.2.2 <i>Road Network Implementation</i>	7
2.3 KAPSCH TRAFFICCOM PROGRESS	10
2.4 AUBURN UNIVERSITY PROGRESS.....	11
2.4.1 <i>Static Testing</i>	11
2.4.2 <i>Dynamic Testing</i>	16
3. FUTURE WORK.....	19
3.1 SRI FUTURE WORK	19
3.1.1 <i>Continued data analysis</i>	19
3.1.2 <i>Software development</i>	19
3.2 PENN STATE FUTURE WORK.....	19
3.2.1 <i>Road Network Implementation</i>	19
3.3 KAPSCH TRAFFICCOM FUTURE WORK	19
3.4 AUBURN UNIVERSITY FUTURE WORK	19
GANTT CHART.....	20

1. Scope

In an open environment, GPS provides a good estimation of vehicle position. Numerous improvements over the basic GPS framework have provided accuracies in the centimeter range. However, blockages of the GPS signal create significant problems for the positioning solution. In so-called “urban canyons”, GPS signals are blocked by the presence of tall buildings. Similarly, heavy foliage in forests can block line-of-sight to the satellites. Because of these problems, a broader approach is needed that does not rely exclusively on GPS. This project takes into account three key technology areas which have each been individually shown to improve positioning solutions where GPS is not available or is hampered in a shadowed environment. First, terrain-based localization can be readily used to find the vehicle’s absolute longitudinal position within a pre-mapped highway segment – compensating for drift which occurs in dead-reckoning system in long longitudinal stretches of road. Secondly, visual odometry keys upon visual landmarks at a detailed level to correlate position to a (visually) premapped road segment to find vehicle position along the roadway. Both of these preceding techniques rely on foreknowledge of road features – in essence, a feature-enhanced version of a digital map. This becomes feasible in the “connected vehicle” future, in which tomorrow’s vehicles have access to quantities of data orders of magnitude greater than today’s cars, as well as the ability to share data at high data rates. The third technology approach relies on radio frequency (RF) ranging based on DSRC radio technology. In addition to pure RF ranging with no GPS signals, information from RF ranging can be combined with GPS range measurements (which may be inadequate on their own) to generate a useful position. Based on testing and characterization of these technologies individually in a test track environment, Auburn will define a combined Integrated Positioning System (IPS) for degraded GPS environments, which will also incorporate ongoing FHWA EAR work at Auburn in fusion of GPS and on-board sensors. This integrated approach will blend the strengths of each technique for greater robustness and precision overall. This research is expected to be a major step forward towards exceptionally precise and reliable positioning by taking advantage of long-term trends in on-board computing, connected vehicles, and data sharing.

1.1 SRI Sarnoff Contribution

The scope of SRI Sarnoff’s work under Year One of this project is the evaluation of their Visual Aided Navigation System for providing highly accurate positioning for vehicles. As such there are 3 major tasks:

- (1) Evaluate and provide a survey of Sarnoff’s existing Visual Navigation results
- (2) Integrate Visual Navigation system on Auburn Engineering’s G35 vehicle test platform and collect test data using the integrated system.
- (3) Process and analyze the data from the tests and evaluate the performance and recommend any improvements and optimizations.

1.2 The Pennsylvania State University Contribution

For sake of clarity and coherence, the scope of Penn State's contribution to the project, as discussed in previous quarterly reports, is reproduced here. The primary objectives under Penn State's purview are:

- (1) Developing the proven particle filter approach so that it can be used for localization with commercial-grade sensors, rather than defense-grade sensors,
- (2) Modifying and optimizing the particle filter algorithm, and exploring alternative approaches, so that localization can take place online (in real-time) rather than offline, and
- (3) Modifying and optimizing the algorithms as well as terrain map representation, so that the localization algorithms work over a large network of roads, rather than a small section of a single road alone.

1.3 Kapsch TrafficCom Inc. Contribution

Kapsch will investigate the accuracy of close proximity calculations available from the 5.9 GHz DSRC communications channel. A great deal of information related to positioning can be inferred from the DSRC communications channel. Basic calculations may provide a location region achieved through the channel ranging calculations to more precise lane based proximity determinations through advanced analysis of the communications channel. Kapsch will research a combination of both approaches through available data defined in the IEEE 802.11p standard for 5.9 GHz communication and through scientific Radio Frequency (RF) analysis.

Kapsch will support Auburn for the characterization of the ability to utilize the 5.9 GHz DSRC communication channel for next generation non-GPS localization services. The Received Signal Strength Indication (RSSI) in-conjunction with other aspects of the DSRC communications channel will be analyzed and a method developed for signal ranging. Kapsch does not believe RSSI ranging techniques will fully meet the desired localization needs. Year 2 will yield more advanced algorithms and DSRC equipment capable of providing lane level localization from the DSRC communications channel. This task includes the following sub-tasks:

- (1) System Engineering and Deployment of DSRC Infrastructure at the Auburn Test Track
- (2) Lab testing of DSRC signal ranging solution
- (3) On-site testing of DSRC signal ranging solution
- (4) Analysis of DSRC signal ranging test results

2. Current Progress

2.1 SRI Progress

2.1.1 Visual Navigation Sensor Package and Data Collection

The sensor package for visual navigation consists of cameras and IMU mounted on the vehicle roof rack, described in a previous report. New data was not collected during the past quarter for processing by SRI Intl.

Figure 1 shows the wiring diagram for the front-only camera system. Three subsystems are shown – a front camera enclosure, a breakout box, and a laptop. The front camera enclosure holds both cameras and the IMU, while the breakout box holds the gigabit Ethernet hub and trigger for the cameras.

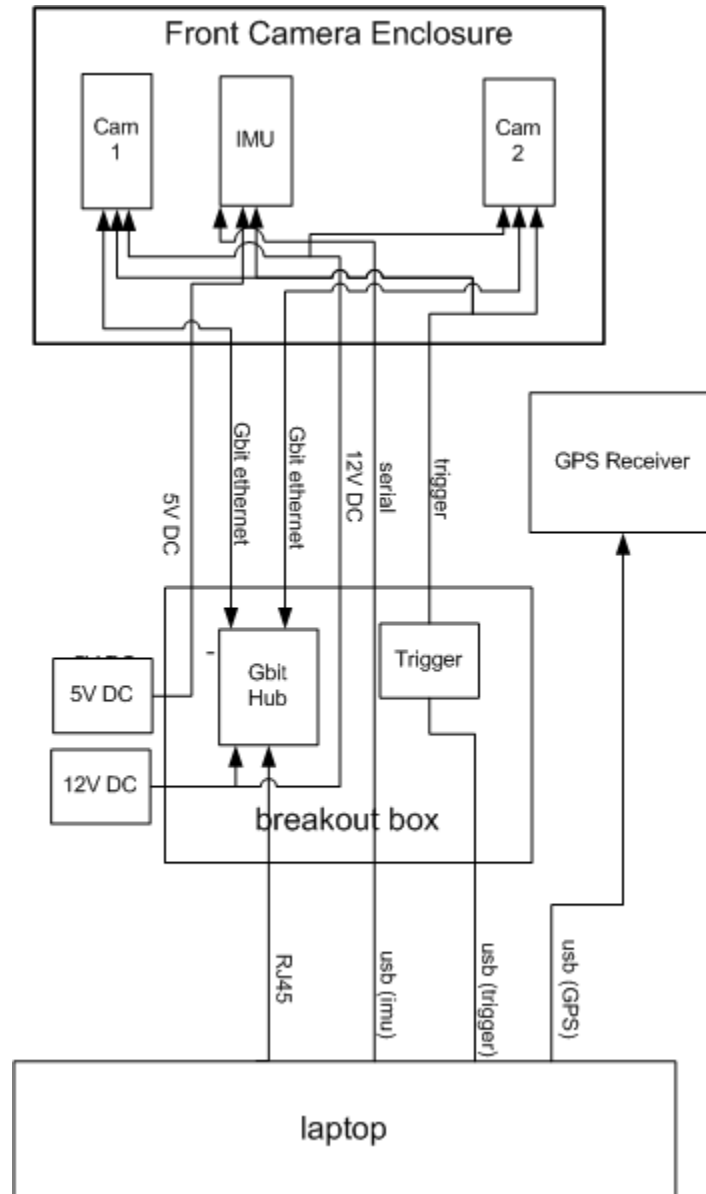


Figure 1: Wiring diagram for the front-only camera system

2.1.2 Extended Kalman Filter Model

Analysis of the Kalman Filter in the visual odometry system has led to a new formulation, which provides a better linearization of the model. This is called the **error state formulation**, and it has the following features:

- Kalman filter estimates errors in the state vector, which are then fed back into the IMU mechanization block to obtain the final corrected navigation solution.

- Circumvents the need to employ platform specific dynamic process model.
- IMU accurately captures the high frequency motion , whereas the indirect Kalman filter operates on the inertial system error propagation equations which evolve smoothly and are much more adequately represented as linear.

An approach called stochastic cloning has also been added to our Kalman filter implementation for visual odometry, which provides better integration of the visual tracking measurements:

- Allows proper treatment of the relative measurements from visual tracking.
- Expresses the relative measurement in terms of motion estimates between the two clone states.
- Enables direct use of relative pose measurements
 - Does not require converting low frequency relative measurements to estimated velocities
- Augments the state vector with two copies of the state estimate, one evolving and one stationary clone
- The evolving clone is propagated by the process model (just like conventional Kalman filter framework) whereas the stationary clone is kept static and does not evolve.
- The relative measurement between the previous and current time instant is then expressed as a function of these two states and a Kalman filter update -modified to incorporate the joint covariance of the two clone states- is performed.

Figure 2 shows the results of the helmet-mounted visual odometry system with a degraded GPS system. The left image shows the estimated positions in a parking lot. The right image shows an example of the improved system with augmented reality.

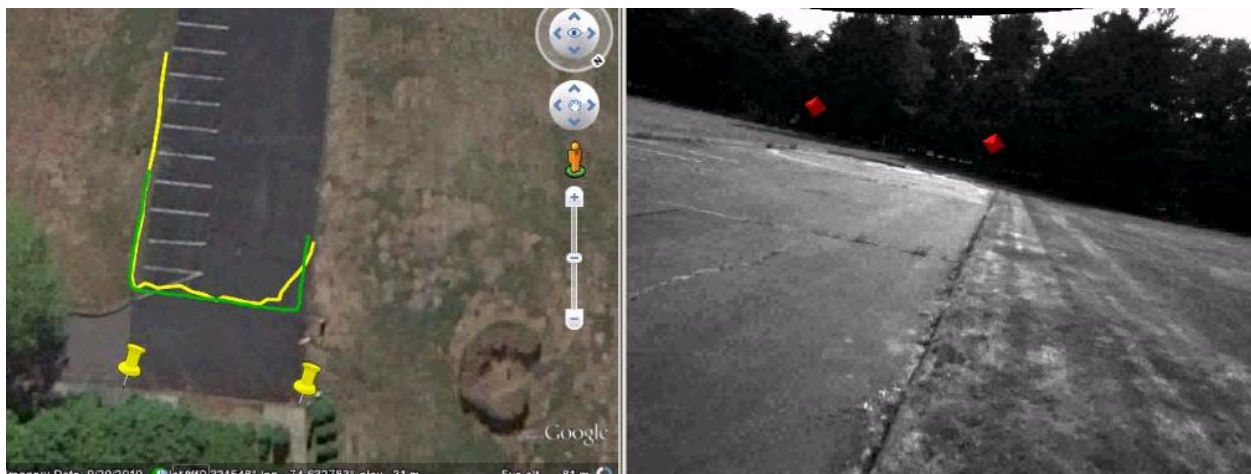


Figure 2: Integration of GPS and visual information is demonstrated using a helmet-mounted visual odometry system with degraded GPS signal. The red dots were inserted into the left image as an example of improved augmented reality.

2.2 Penn State Progress

2.2.1 Real-time Implementation

Task (2) entailed the development of a real-time implementation of the terrain-based localization algorithm. The task was completed in this quarter and the algorithm was delivered to Auburn University. We are currently assisting our colleagues at Auburn University in understanding and integrating the localization algorithm into the Integrated Positioning System (IPS). As part of Task (3), Penn State has demonstrated the applicability of the algorithm at a simulated T junction. The details of the progress since the previous quarterly report and current and upcoming work are included in the following sections.

2.2.2 Road Network Implementation

Task (3) aims at expanding the scope of the terrain-based localization algorithm so that it may be used across an entire road network. As part of this task, Penn State has modified the algorithm to suit a scenario where multiple road segments may be part of a vehicle's travel path. Specifically, data from a T-junction was used in a simulation where the vehicle could either go straight or take a right turn. This scenario is depicted in Figure 3. The corresponding terrain maps are included in Figure 4.

The figures below show the T junction simulation for the road network implementation. The figure on the left (Figure 3) shows a bird's eye view of the T-junction. The figure on the right (Figure 4) shows the terrain maps with pitches. At the point with the intersection, the terrain maps diverge.

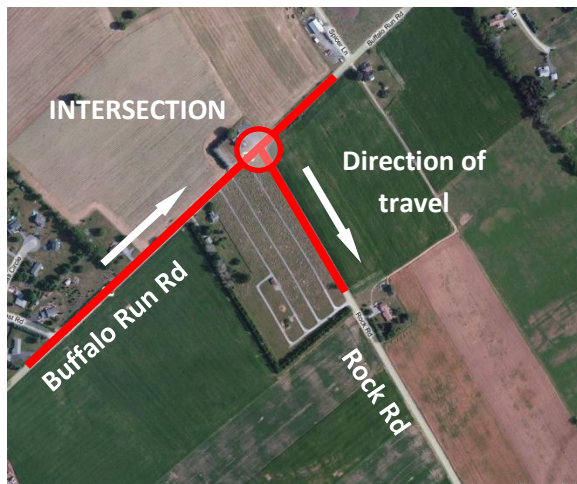


Figure 3: T junction used for simulation. Vehicle can either go straight on Buffalo Run Rd or take a right turn onto Rock Rd.

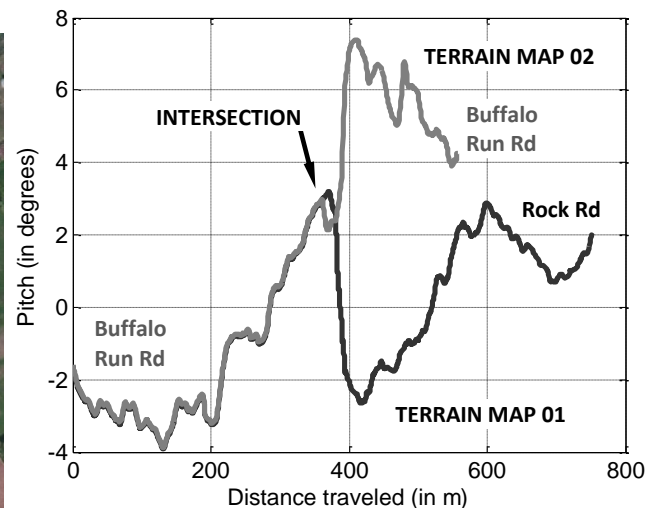


Figure 4: Terrain maps depicting pitch values for the two possible paths that the vehicle can take at this T junction.

A multiple model estimation scheme was adopted to handle the multiple travel paths possible in this scenario. Specifically, two estimators were included in the Simulink model to provide position and covariance estimates for each of the two possible travel paths. Next, the observed and predicted pitch values were used to determine the probability of the vehicle being on either road segment according to the following equation:

$$P_k(\text{Road } i) = \frac{P_{k-1}(\text{Road } i) \cdot \text{Likelihood}(\theta_k | \hat{\theta}_k^i)}{\sum_j P_{k-1}(\text{Road } j) \cdot \text{Likelihood}(\theta_k | \hat{\theta}_k^j)}$$

where $P_k(\text{Road } i)$ represents the probability that the vehicle is on road segment i at time k , θ_k represents the pitch measurement obtained at time k , and $\hat{\theta}_k^i$ represents the predicted value of pitch at time k if the vehicle was on road segment i . The likelihood is calculated assuming a Gaussian distribution of the pitch values with mean $\hat{\theta}_k^i$. The variance of the Gaussian distribution is determined from the pitch values at the sigma points at time k (obtained from the Unscented Kalman Filter).

Preliminary results indicate that the multiple model estimation scheme is able to correctly identify the road segment, and local tracking in the absence of GPS is still achieved. Figures 5 and 6 depict the possible travel paths (corresponding to Terrain Maps 01 and 02). Figure 7 (left) represents the tracking error when Estimator 1 assumes that the Terrain Map 01 is the true representation of the terrain the vehicle is currently traveling over. Figure 7 (right) represents the tracking error when Estimator 2 assumes that the Terrain Map 02 is the true representation of the current terrain. It must be noted that both estimators run simultaneously in the simulation.

The figures below show the GPS coordinates in latitude and longitude of the travel path for the intersection with the various terrain maps (Terrain Map 01 (left – Figure 3), and Terrain Map 02 (right – Figure 6)). Figure 7 shows the tracking error for Terrain Map 01, and the error stays below 3 m. Figure 8 shows the tracking error for Terrain Map 02, and the error increases dramatically. These figures show how the vehicle knows which direction the vehicle has traveled.

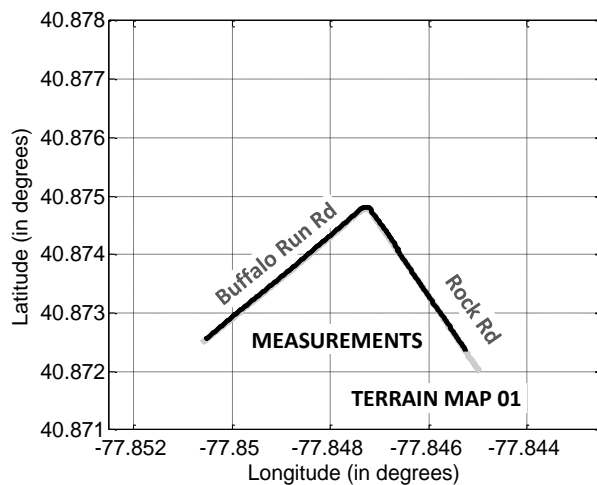


Figure 5: GPS coordinates of Terrain Map 01 (grey). The actual travel path (black) corresponds to Terrain Map 01, i.e. the vehicle took a right turn on to Rock Rd.

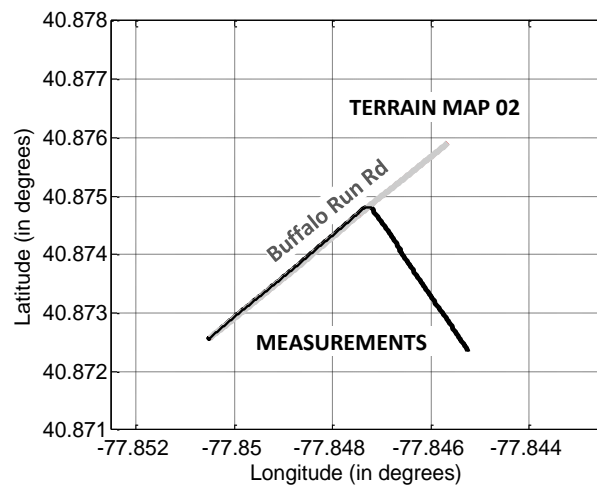


Figure 6: GPS coordinates of Terrain Map 02 (grey). The vehicle (black) did not go straight on Buffalo Run Rd.

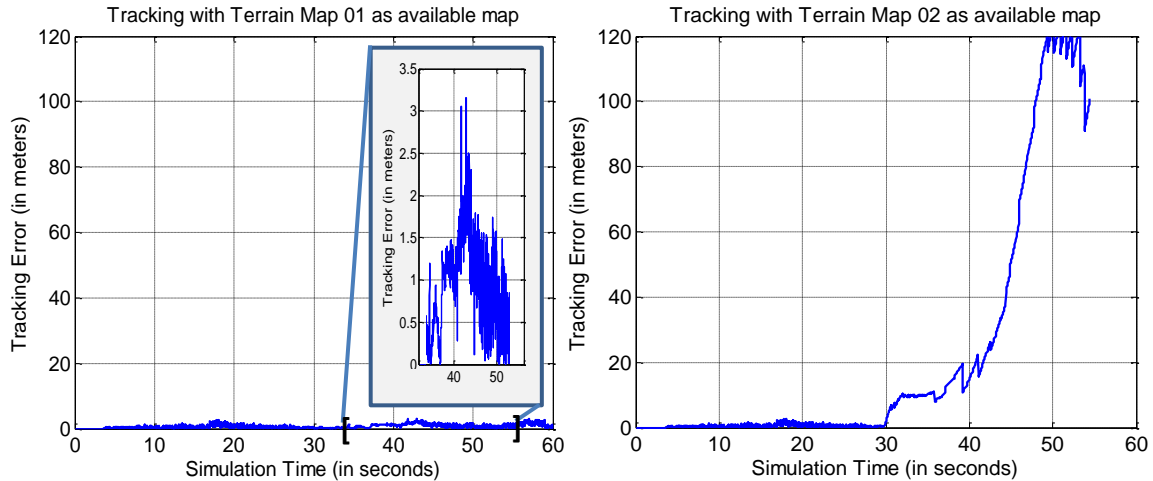


Figure 7: Tracking error with Estimator 1, assuming Terrain Map 01 is the true representation of current terrain (left) Tracking error with Estimator 2, assuming Terrain Map 02 is the true representation of current terrain(right)

Figure 8 denotes the probabilities for each terrain map being the true representation of the terrain. It is observed that before reaching the intersection, the probabilities for both terrain maps is 0.5 since they represent the identical terrain as evinced by Figure 4. After reaching the intersection (at approximately 30 seconds into the run), the probability that the terrain map in Estimator 1 is correct increases to 1, whereas the probability that the terrain map in Estimator 2 is correct reduces to zero. Now the position estimate from Estimator 1 is provided to the IPS for fusion with other position estimates.

Figure 8 shows the probability for each Terrain map. The probability stays at .5 until the point of the intersection, at which time the probability increases to 1 (for Terrain Map 01) or 0 (for Terrain Map 02).

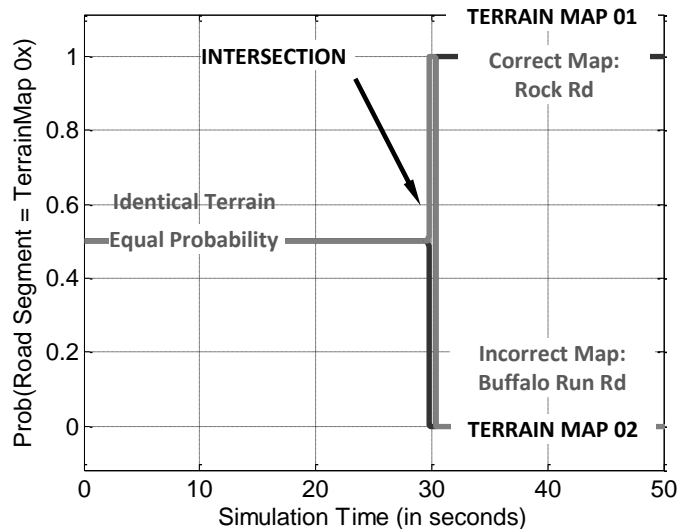


Figure 8: Probability that Terrain Map 0x is the correct map. Position estimates from road segments with high probability are chosen to be fed to the IPS

2.3 Kapsch TrafficCom Progress

In November 2010 Auburn research team requested Kapsch for guidance on how the positioning experiment can utilize a different method of wireless ranging.

The originally proposed research approach for the Year 1 research was based on measurements of the Receiver Signal Strength Indicator (RSSI). The RSSI would be measured by an in-vehicle DSRC on-board unit (OBU) using a signal transmitted by a 5.9GHz DSRC roadside unit (RSU). Since the RSSI measurements are related to the RSU signal strength measured by the OBU, it was expected that the RSSI could estimate the relative distance between the OBU and the RSU.

However, Auburn earlier reported results showed that RSSI measurements are not sufficiently accurate to be used as a ranging parameter.

Instead of the RSSI approach, Auburn research team proposed to use a different approach based on the wireless packet “time-of-flight”. Results published by other researchers showed merits to such an approach.

The “time-of-flight” approach requires measurements of a time delay for a packet transmitted between an RSU and an OBU. The time delay between transmission and reception of a wireless packet is extremely small. For a typical test distance of several hundred meters the time delay is estimated to be in sub-microsecond range.

In January 2011, Kapsch team responded with a tentative design. Kapsch proposed to measure the “time-of-flight” during a dual exchange of messages between an RSU and OBU (Figure 9). The “time of flight” is measured between a transmission of a packet from an OBU to RSU at time t_1 , and a reception of an acknowledgment packet by the OBU at t_2 .

Figure 9 shows the time of flight experiment to improve ranging measurements. Two systems are shown, the OBU radio and the RSU radio. At t_1 , the packet is sent to the RSU radio. At t_2 , the acknowledgment is sent back from the RSU radio to the OBU radio.

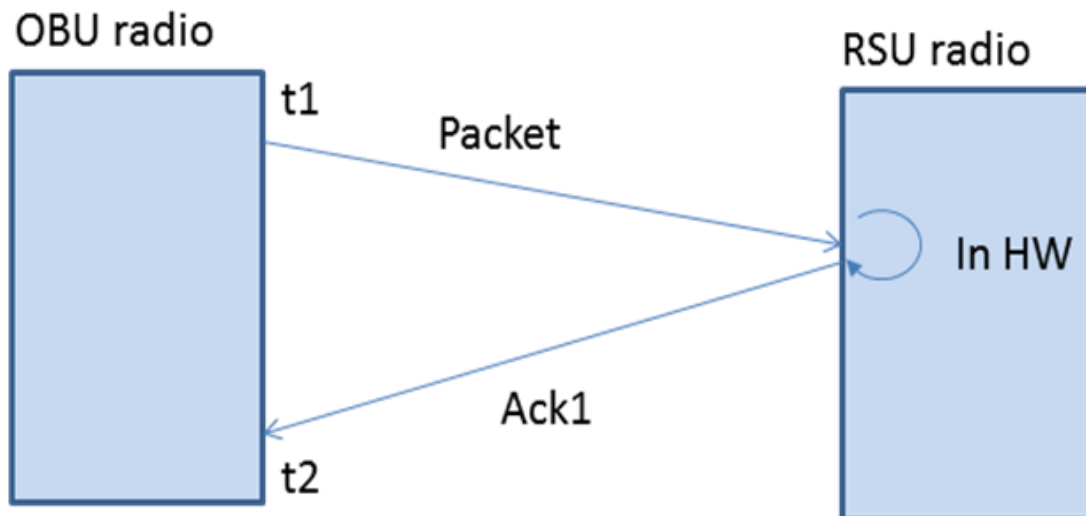


Figure 9: Time-of-Flight Experiment

Kapsch proposed to create a special OBU by modifying one of its commercial products to enable the use of a high-resolution internal clock timer to measure the delay t_2-t_1 . Kapsch will also provide updated radio software for the OBU which can measure the time-of-flight.

2.4 Auburn University Progress

Auburn has interfaced the Kapsch ranging system with the IPS framework, and a test was conducted at Auburn's NCAT test facility to determine if the distance between two DSRC radios can be obtained using the time of arrival technique. To determine this, the output of the receiver radio was collected at different distances from the base station radio along with differential GPS data for truth using the IPS framework. No attempt was made at resolving time of flight units with actual distances.

The ranging test was performed using our research vehicle, which is equipped with Novatel Differential GPS and a DSRC on-board unit. The onboard GPS and DSRC antenna were placed on the roof of the vehicle. The base station DSRC antenna was placed at roughly the same height as the vehicle. Both radios were configured by following the guide that Kapsch had provided. Using the Auburn's interface to Mission Oriented Operating Suite (MOOS), the range measurement from the DSRC radio and the position data from the Novatel GPS receiver was collected and recorded. The test consisted of the static and dynamic portions. For the static tests, the vehicle was moved to the various positions around the skid pad and held stationary when the tests were running. During the dynamic tests, the vehicle was driven around the skid pad area of NCAT test track to vary the distance between the vehicle and the base station DSRC antennas. Clear line of sight for DSRC antennas was ensured for several of the test runs to avoid possible signal loss, while other tests intentionally had obstacles blocking line-of-sight. After collecting the data, the position of the base station was recorded using Novatel DGPS. Truth distance was obtained using the distance from the GPS position of the base station to the position of the receiver on the antenna. Truth data shows precision within 2 centimeters.

2.4.1 Static Testing

Static tests were performed from various distances – 4.5m, 35m, 63m, and 72m. The results are shown in Figures 10-17. Table 1 shows the mean and the standard deviation of the time of flight values from various distances.

Figure 10 shows the close range (4.5m) static range test. The time of flight measurement alternates between 702 and 703.

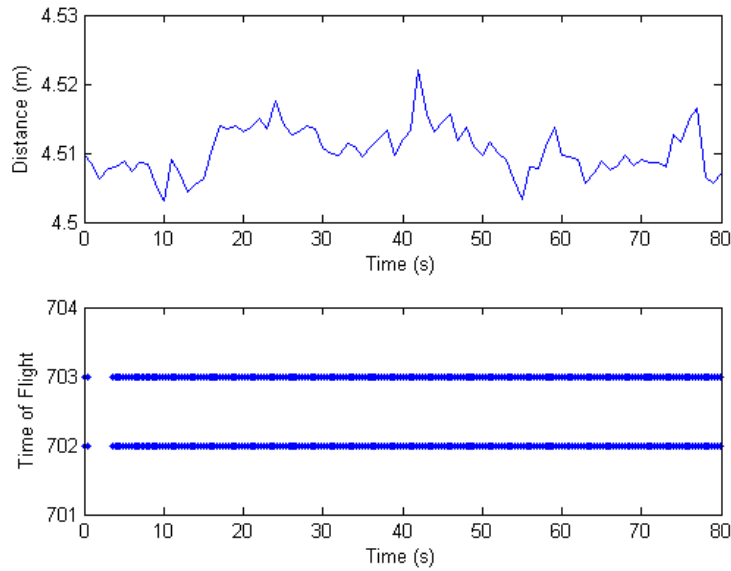


Figure 10: Close Range Static Test Result

Figure 11 shows the histogram for the close range static test. In this test, the 702 measurement occurs about 7500 times, while the 703 measurement occurs slightly more than 25000 times.

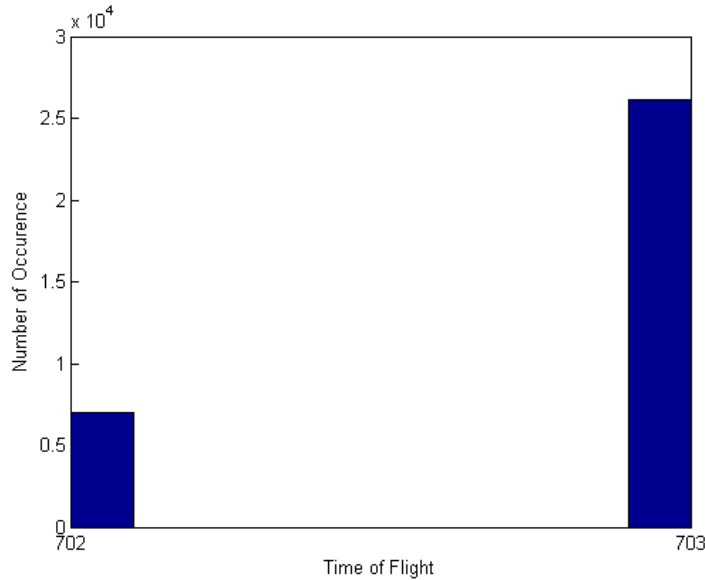


Figure 11: Close Range Static Test Histogram

Figure 12 shows the results for the medium range (35m) static test result. The time of flight measurements alternated between 3 values – 703, 704, and 705.

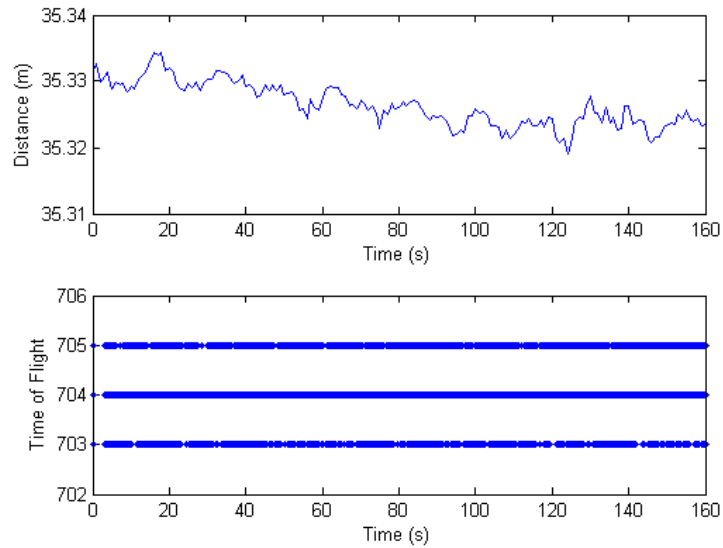


Figure 12: Medium Range Static Test Result

Figure 13 shows the histogram for the medium range test histogram. The 703 measurement occurred about 4000 times, the 704 measurement occurred about 60000 times, and the 705 measurement occurred about 5000 times.

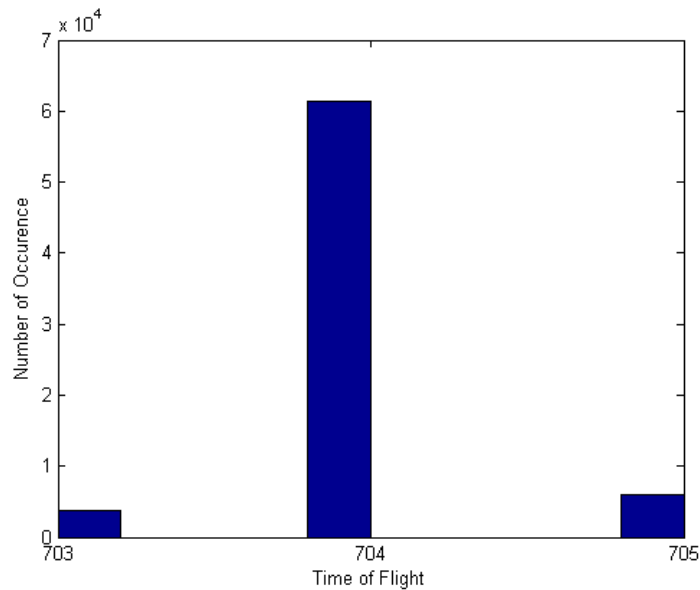


Figure 13: Medium Range Static Test Histogram

Figure 14 shows the long range (63m) test results. The long range results alternated between several values – 701,702,703,704,705, 706, and 708.

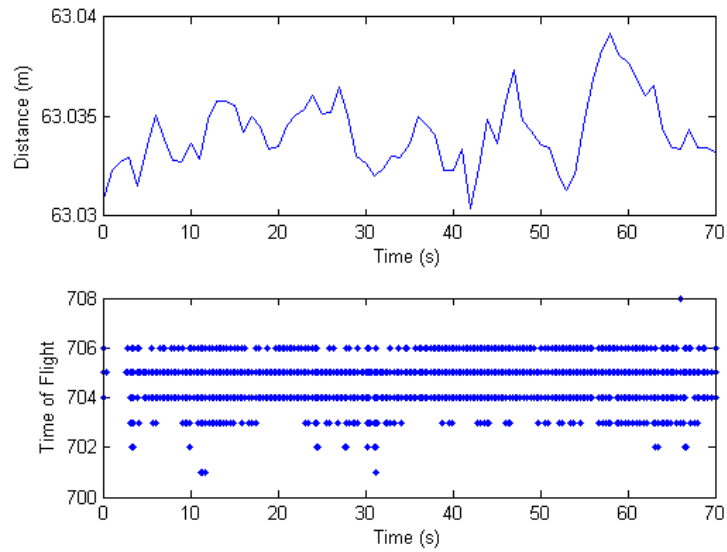


Figure 14: Long Range Static Test Result

Figure 15 shows the histogram for the long range test. The outlying values, 701,702, and 708, occurred rarely, while 703 occurred about 500 times. 706 occurred about 1500 times, while 704 occurred 3000 times. The most occurrences happened for 705, with 9000.

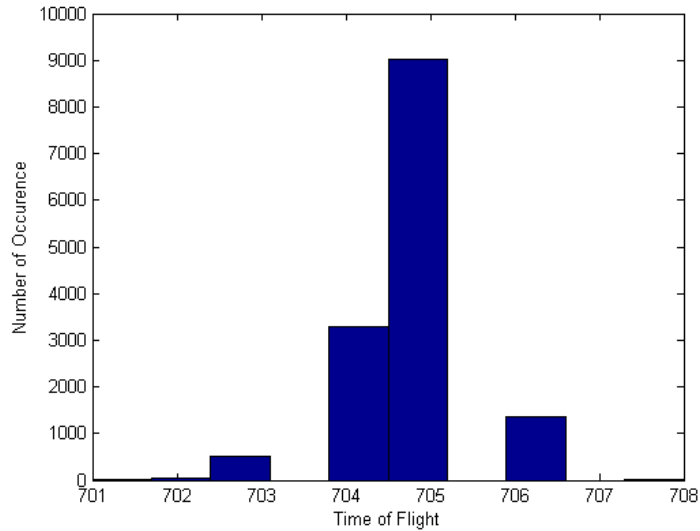


Figure 15: Long Range Static Test Histogram

Figure 16 shows the maximum range (72m) test. Beyond this range, data could not be collected or only very rarely was detected. Like the long range set, the measurements occurred over a range of time of flight values (701 – 707).

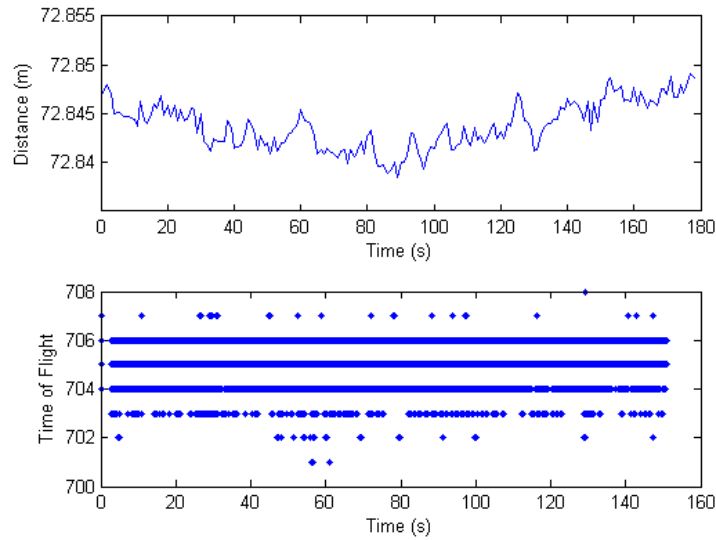


Figure 16: Maximum Range Static Test Result

Figure 17 shows the histogram for the maximum range test. The maximum number of occurrences was 705 with 33000 occurrences, followed by 706 with 20000 occurrences. The other time of flight measurements had less than 10000 occurrences.

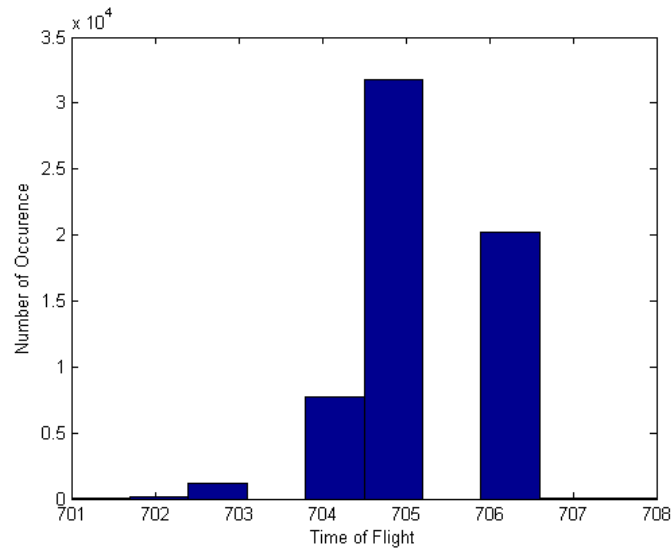


Figure 17: Maximum Range Static Test Histogram

Table 1: Means and standard deviations for the time of flight

Test Range (m)	Mean	Std. Deviation
4.5	702.7899	0.4074
35	704.0324	0.3703
63	704.7769	0.6896
72	705.1634	0.7277

2.4.2 Dynamic Testing

Dynamic testing was conducted to determine the performance of the system while the vehicle is moving. On the first test run, the vehicle was driven away from the base station and maintained line-of-sight. At the end of the skid pad area, the vehicle was put in reverse and driven back to near the starting position, as seen in Figure 18.

Figure 18 shows the GPS position of the vehicle and the base station for the first dynamic test. The path of the vehicle consisted of driving about 60 meters, followed by reversing. At the end of the run, the vehicle differed from its starting position by about 5 meters.

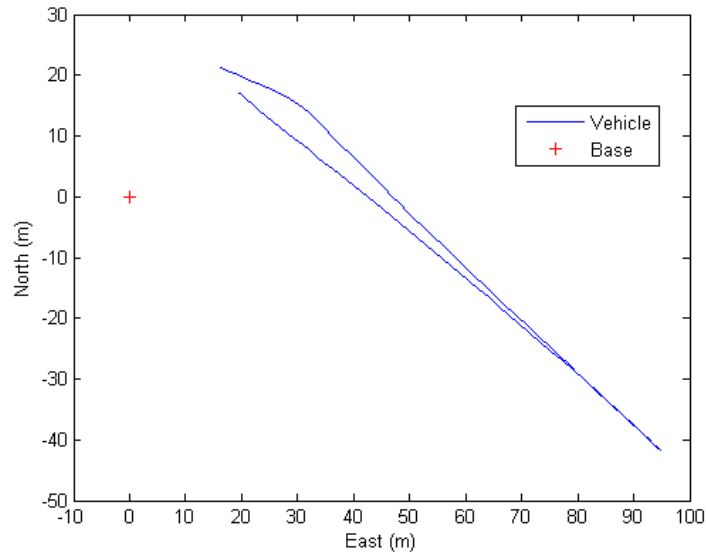


Figure 18: GPS position of the vehicle and the base station

The result of this run can be seen in Figure 19. The signal flight time increased as the distance between the antennas increased. Also, the flight time changed by 1 for about every 13 meters of distance.

Figure 19 shows the distance and ranging output vs. time for the first dynamic maneuver. The ranging output followed roughly the same peak shape as the distance, with a variation of about 2-3 time of flight values throughout.

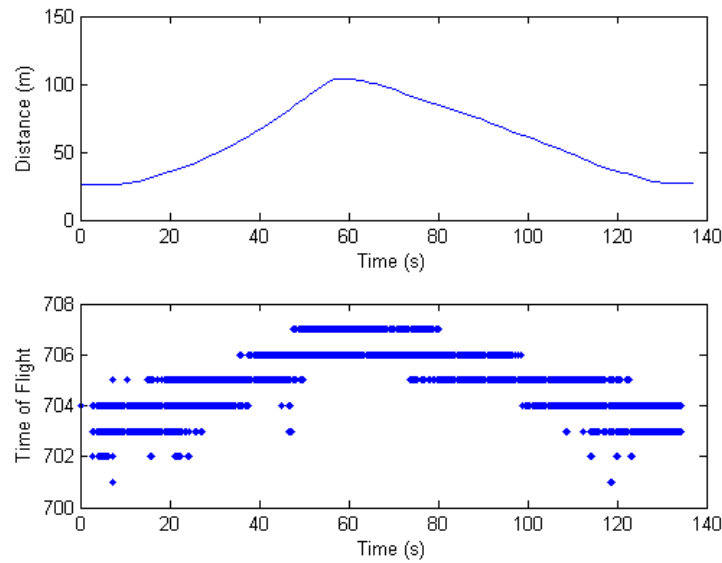


Figure 19: Distance and ranging output vs. time

On the second test, the vehicle was driven outside of the skid pad to provide a larger distance between the radios. In this test, line-of-sight was not maintained due to trees and large rock piles present on the skid pad. The vehicle path and the output result can be seen in Figure 20 and 21, respectively. The vehicle began at the base station (red plus) and traveled counterclockwise to the easternmost part of the path. At this point, the car was put in reverse until the looped portion, where it was put in drive and the loop completed. Along the reversed region to the east of the loop, trees were present. Also, two rock piles blocked line of sight along the southernmost path of the vehicle.

Figure 20 shows the GPS position of the vehicle and base station for the second maneuver. The vehicle was driven down off of the skidpad towards to exit road. The vehicle was then stopped, put in reverse for about halfway down the road, then put back into drive and looped to the starting position.

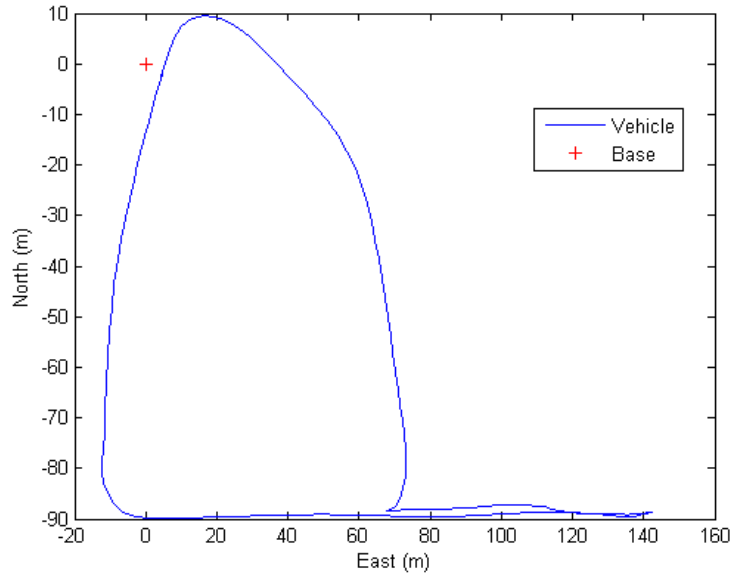


Figure 20: GPS position of the vehicle and the base station

Figure 21 shows the time of flight and distance measurements for the second dynamic test. The shape of the ranging output does not correlate well with the distance; however, due to a treeline as well as large piles of rock at the test site, the measurements were probably corrupted.

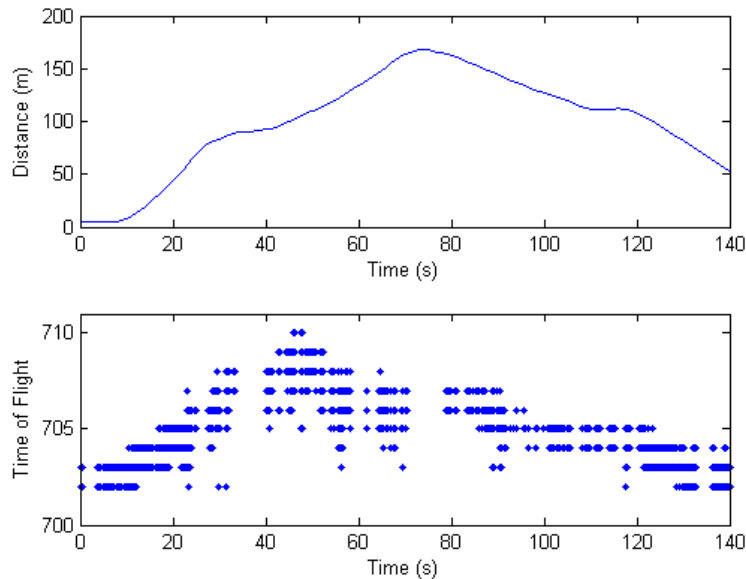


Figure 21: Distance and ranging output vs. time

Due to the rock piles blocking the line of sight of radios, the ranging measurements were lost around 30 seconds and 75 seconds into the test.

The results of this test run were sent to Kapsch, and the results agreed with what they had seen in their own tests. With the inclusion of the interface to Kapsch complete, all subsystems are now integrated into Auburn's data collection and processing system.

3. Future Work

3.1 SRI Future Work

3.1.1 Continued data analysis

- Adding Landmark matching to pose pipeline; combining GPS and Landmarks in filter.

3.1.2 Software development

- Output pose in NED instead of UTM coordinate frame. Improvement of GPS alignment algorithms.

3.2 Penn State Future Work

3.2.1 Road Network Implementation

The current setup included only short road sections (up to 5 km) and the entire terrain map could be loaded into the memory. For large road networks, however, the data will have to be stored separately and accessed as per the clients' requests, the clients being the estimators associated with each possible travel path. Penn State is currently in the process of setting up an ad-hoc onboard server to handle requests for terrain data.

Penn State's plans for the immediate future include setting up an ad-hoc on-board server for terrain database management. Penn State's plans for the near future include mapping roadway networks in the State College area to generate a representative road network terrain map. This will be followed by field tests to check the efficacy of the algorithm with various intersection scenarios.

3.3 Kapsch TrafficCom Future Work

The Kapsch design work to make changes to the hardware and software is estimated to last 1-1.5 calendar month. Kapsch development team plans to conduct initial tests in the lab to confirm the technical feasibility of the approach and then provide Auburn necessary hardware and software to conduct the testing on the test track.

3.4 Auburn University Future Work

Auburn will continue to work on the IPS as well as conduct testing for each of the subsystems, as needed. Auburn will also be preparing for its test on the Detroit test track in November.

Gantt Chart

As indicated in the Schedule for Year 2, the Gantt chart has been refined to reflect realistic timetables, most notably the demonstration of the system in winter.

	September	October	November	December	January	February	March	April	May	June	July	August
Schedule (Proposal)												
1.0 Project Management	█	█	█	█	█	█	█	█	█	█	█	█
1.1 Team Meetings												
1.2 Conduct Expert Panel Mtgs				█								
2.0 Literature Survey												
3.0 Investigate Terrain-Based Localization	█	█	█	█	█	█	█					
3.1 Install on Test Vehicle	█	█	█	█	█	█	█					
3.2 Define Test Protocol												
3.3 Collect Characterization Data and Analyze Results												
4.0 Investigate Visual Odometry Based Positioning												
4.1 Install on Test Vehicle												
4.2 Define Test Protocol												
4.3 Collect Characterization Data and Analyze Results												
5.0 Investigate DSRC-based RF Ranging												
5.1 Install DSRC Equipment on Test Vehicle and Test Track												
5.2 Define Test Protocol												
5.3 Collect Characterization Data and Analyze Results												
Milestone 1: Testing and Analysis Completed for Each Positioning Technique												
6.0 Define Integrated Positioning System												
6.1 Define Initial IPS												
Milestone 2: Define Initial Integrated Positioning System												
6.2 Revise IPS Definition Based on Expert Panel Feedback								█				
7.0 Demonstration and Final Report												
7.1 Demonstrate Vehicle Capability												
7.2 Develop Transition Plan												
7.3 Deliver Final Report												